Int. J. Chem. Sci.: 13(4), 2015, 2039-2048
ISSN 0972-768X
www.sadgurupublications.com

SYNTHESIS, STRUCTURAL AND OPTICAL PROPERTIES OF L-VALINE MODIFIED ZnO NANOPARTICLES

R. P. GANORKAR[a], K. P. KALKAR[a] and Y. S. TAMGADGE[*]

Department of Physics, Mahatma Fule Arts, Commerce & Sitaramji Chaudhari, Science
Mahavidyalaya, WARUD – 444906, Dist. Amravati (M.S.) INDIA
[a]Department of Chemistry, Mahatma Fule Arts, Commerce & Sitaramji Chaudhari Science
Mahavidyalaya, WARUD – 444906, Dist. Amravati (M.S.) INDIA

ABSTRACT

Zinc oxide (ZnO) nanoparticles (NPs) have been synthesized by co-precipitation method using various concentrations of L-valine as surface modifying agent. All these samples of ZnO NPs were calcined with slow heating rate at 600^0C for two hours for the removal of L-valine. UV-visible spectroscopy has been utilized to characterize calcined and uncalcined ZnO NPs. Fourier transform infra-red spectroscopy confirmed the role of L-valine as surface modifier. Particles sizes of all uncalcined and calcined NPs have been calculated using Effective Mass Approximation method. ZnO NPs capped with L-valine before calcination exhibit very narrow particle size distribution (7 to 8 nm) whereas particle size increased (upto 18 nm) after removal of L-valine through the process of calcination. In both uncalcined and calcined ZnO NPs, particle size decreased for ZnO NPs synthesized using largest concentration of L-valine. X-ray diffraction analysis confirms the formation of pure phase wurtzite hexagonal ZnO NPs. Morphological studies have been performed using field emission scanning electron microscopy and transmission electron microscopy techniques.

Key words: UV-visible spectroscopy, ZnO nanoparticles, X-ray diffraction.

INTRODUCTION

Particles in nano range have high surface to volume ratio and show very interesting properties, which are of scientific and technological importance[1-7]. Zinc oxide is very interesting and promising material because of its wide band gap nature, natural abundance and non-toxicity. Band gap may be further increased as we decrease the particle size. These wide band gap nanostructured ZnO semiconductor materials show promising applications in nonlinear optics, optoelectronic devices, sensors devices etc.[8-13]. ZnO has a room temperature band gap of 3.3 eV and high exciton binding energy of 60 meV. It has got

---

[*] Author for correspondence; E-mail: ystamgadge@gmail.com

technological importance because of its high mechanical and chemical stability, good optical and thermal properties in addition to its natural abundance and non-toxicity. ZnO nanoparticles (NPs) can be synthesized by various methods, among which polyol or amino acid assisted synthesis technique is mostly favored[14]. Surface modifying agents have very important role in controlling the particle size and in avoiding the agglomeration of NPs. After successful synthesis of de-agglomerated NPs, surface modifiers can be removed by the process of calcination at slow heating rate by which de-agglomerated nanostructures can be retained.

Amino acids belong to an important class of water soluble organic surface modifying agents that play critical role in the synthesis of narrow range NPs. They are commercially available, inexpensive and non-biohazard materials. Researchers have demonstrated the use of L-histidine and L-cysteine as capping agents for semiconducting nanomaterials. We have used amino acids as a capping agent in our previous works[15-18]. The amino group has a loan pair of electrons and capable of forming hydrogen bonds[19,20].

In this paper, we report synthesis of ZnO NPs by using L-valine as surface modifying agent. ZnO NPs with particle size of 7 nm can be effectively synthesized by using L-valine. These NPs were calcined at 600°C for the removal of capping agent. Effect of presence and absence of capping agent is studied by characterizing uncalcined and calcined ZnO NPs by UV-visible spectroscopy. Powder X-ray diffracttometry (XRD) has been utilized for the structural evaluation of ZnO NPs. Morphological studies have been performed using field emission scanning electron microscopy (FESEM) and transmission electron microscopy (TEM).

EXPERIMENTAL

Synthesis of ZnO NPs

ZnO NPs were synthesized using co-precipitation method. All chemicals used were of analytical reagent grade and used without further purification. Zinc chloride ($ZnCl_2$) AR grade and sodium hydroxide pellets (NaOH) AR grade were procured from SD-fine Chemicals, Mumbai. L-valine was purchased from Sigma Aldrich, USA.

Firstly, solutions of 1M $ZnCl_2$, 2M NaOH and 1M L-valine were prepared in double distilled water in separate beakers. Double distilled water was used as a solvent for the synthesis of ZnO NPs. Then four samples of ZnO NPs containing different concentrations of L-valine capping agent were prepared. For synthesis of pure ZnO NPs (sample name ZnO-Pure), 5 mL of 1M $ZnCl_2$ was dissolved into 100 mL double distilled water and it was stirred for 30 min using magnetic stirrer at room temperature. Then 5 mL of 2 M NaOH was added drop wise into this solution, which immediately resulted into white precipitate. ZnO NPs capped with L-valine has been synthesized by adding and stirring L-valine before addition of NaOH in the solution. Three such samples were synthesized by adding 1 mL (sample name ZV1), 2 mL (sample name ZV2) and 5 mL (sample name ZV5) L-valine into the solution and precipitate were recovered after drop by drop addition of NaOH.

The precipitate was then separated using centrifuge machine at 4000 rpm (REMI Model-4RC) for 30 min and washed 2-3 times with double distilled water. White precipitate was dried in an electric oven at 100°C for 2 hrs and fine particles were obtained after grinding in agate mortar. Table 1 shows the samples prepared by using different concentrations of L-valine. All samples were calcined in the muffle furnace at 600°C for 2 hrs.

Table 1: Details of synthesized ZnO NPs

Sample name	$ZnCl_2$ 1M	NaOH 2M	L-valine 1M	State of sample
ZV1	5 mL	5 mL	1 mL	Uncalcined
ZV2	5 mL	5 mL	2 mL	Uncalcined
ZV5	5 mL	5 mL	3 mL	Uncalcined
ZV1C	5 mL	5 mL	1 mL	Calcined at 600^0C
ZV2C	5 mL	5 mL	2 mL	Calcined at 600^0C
ZV5C	5 mL	5 mL	3 mL	Calcined at 600^0C

Characterization

All samples of ZnO NPs were subjected to structural and morphological characterization by X-ray diffraction (XRD) using Rigaku diffractometer Miniflex II with nickel filtered CuK_α radiation (λ=1.5406 Å) at a scan rate 0.50 min^{-1} and angle 2θ ranging from 10 to 70°; transmission electron microscopy (TEM) using JEM-2100 HR-TEM (Make-JEOL, Japan; operating voltage 200kV) and field emission scanning electron microscopy (FE-SEM) using Hitachi S-4800, Japan at an operating voltage 15kV. Ultraviolet-visible (UV-vis) spectroscopy was performed using UV-visible spectrophotometer (BLK-C-SR, Stellarnet, USA) in the wavelength range 190-1100 nm. Fourier transform infra-red (FT-IR) spectra were recorded using IR double beam spectrophotometer, 8400S-Shimadzu, Japan.

RESULTS AND DISCUSSION

UV-visible study

Figs. 1 and 2 show UV-visible spectra for calcined and uncalcined samples of ZnO NPs as described in Table 1. From the figure, it is evident that maximum absorption takes place at 346 nm, 344 nm and 341 nm for the uncalcined samples ZV1, ZV2 and ZV5, respectively. Maximum absorption peak shifts towards ultraviolet region as the concentration of capping agent was increased. Thus, use of capping agent in controlling the particle size is evident. Calcined samples also follow the same trend of increased band gap and decreased particle size for ZnO NPs synthesized using largest concentration of L-valine. Increase in the band gap gives clear indication of formation of nanoparticles. In case of calcined NPs, maximum absorption peaks shit towards higher wavelength, which is evident from Fig. 2. The particle size is calculated from UV-visible spectra by using effective mass approximation (EMA)[21]. The EMA formula can be stated as:

$$E_g = E_{bulk} + \frac{h^2}{8r^2}\left(\frac{1}{m_e^*} + \frac{1}{m_h^*}\right) - \frac{e^2}{4\pi\varepsilon_o\varepsilon_r\gamma_e} \quad \ldots(1)$$

Where E_g is band gap energy for NP, E_{bulk} is energy gap for bulk semiconductor, m_e^* and m_h^* are effective electron and hole mass (for ZnO, $m_e^* = 0.19\ m_0$, $m_h^* = 0.21\ m_0$). γ_e is Bohr exciton radius, ε_r is relative dielectric constant and ε_o is dielectric constant of air. Data calculated from EMA model is summarized in Table 2.

Table 2: Optical data calculated from UV-visible spectra of calcined and uncalcined ZnO NPs

Sample name	Particle Size (nm)		
	EMA model	XRD	TEM
ZnO-Pure	20		
ZV1	8		
ZV2	7.5		
ZV5	7	8	7
ZVC1	13		
ZVC2	16		
ZVC3	18	21	

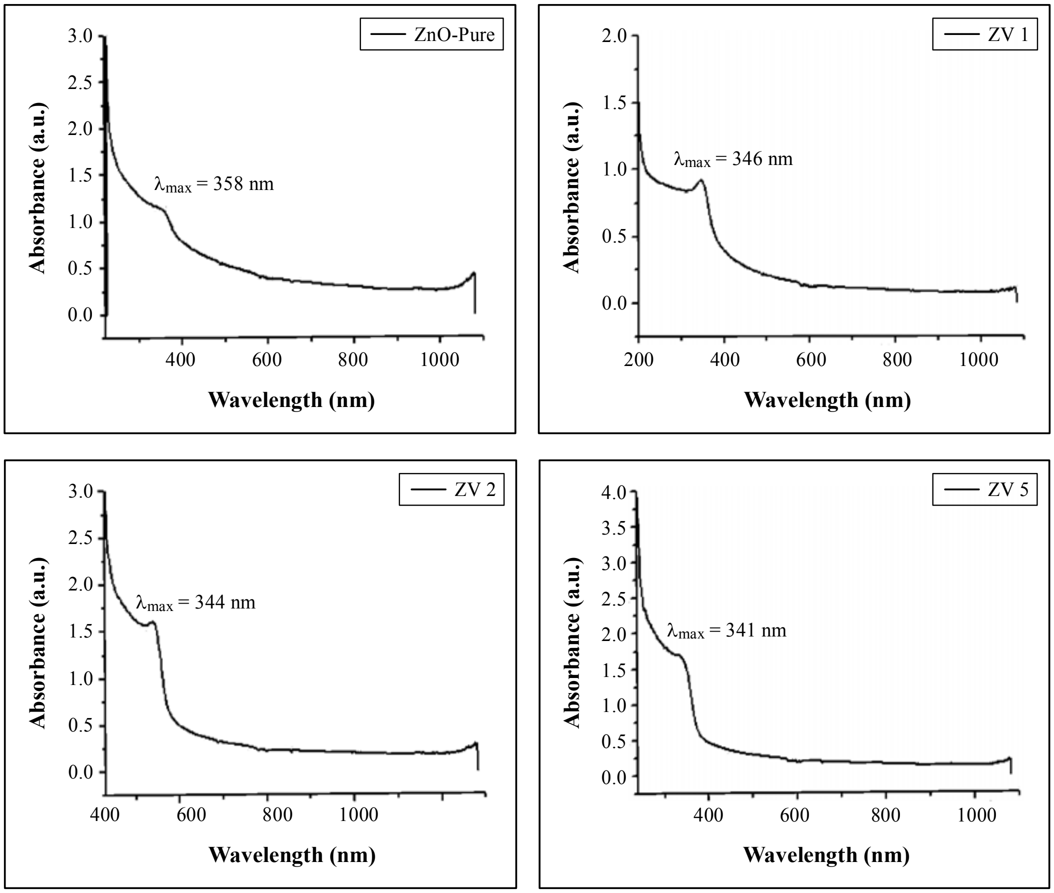

Fig. 1: UV-visible spectra of uncalcined ZnO NPs

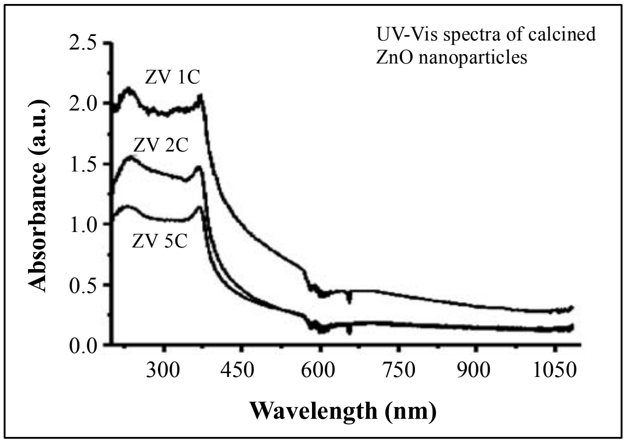

Fig. 2: UV-visible spectra of calcined ZnO NPs

FT-IR spectroscopy

The functional groups and bonding structure of ZnO NPs capped with L-valine samples were investigated by FT-IR spectroscopy. The FT-IR spectrum has been recorded using powder KBr pellet method. Small fraction of powder sample of ZnO NPs capped with L-valine (sample ZV5) is mixed with KBr and a pellet is formed. The pellet is subjected to IR measurements. Fig. 3 shows FT-IR spectra of ZnO NPs capped with L-valine. Peaks assignments are summarized in the Table 3[22,23].

Table 3: FT-IR peak assignments

Peaks (cm^{-1})	Assignments
3221	Asymmetric CH_2 stretching
2109	Combination of CH_3 bending
1400	HCH bending
1085	CH_3 bending
1029	CH_3 bending
846	OH torsional bending
773	CO_2 bending
712	C-C stretching, C=O bending

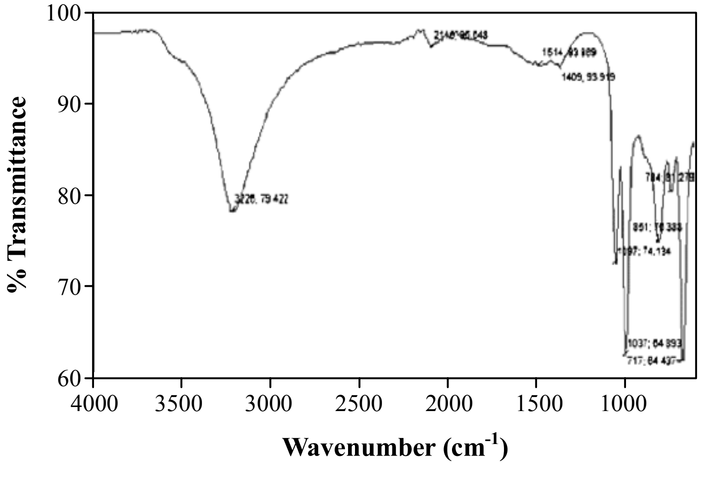

Fig. 3: FTIR spectrum of L-valine capped ZnO NPs

Structural studies using XRD

Figs. 4 and 5 show XRD pattern of uncalcined and calcined ZnO NPs. All diffraction peaks can be indexed in hexagonal crystal structure with cell parameter a = 3.264 Å and c = 5.219 Å (JCPDS file No. 79-0208). The peaks obtained at 2θ° values of 31.62, 34.33, 36.12, 47.33, 56.31, 62.64, 66.03, 67.64, and 68.73 can be attributed to the planes (100), (002), (101), (102), (110), (103), (200) and (112), respectively.

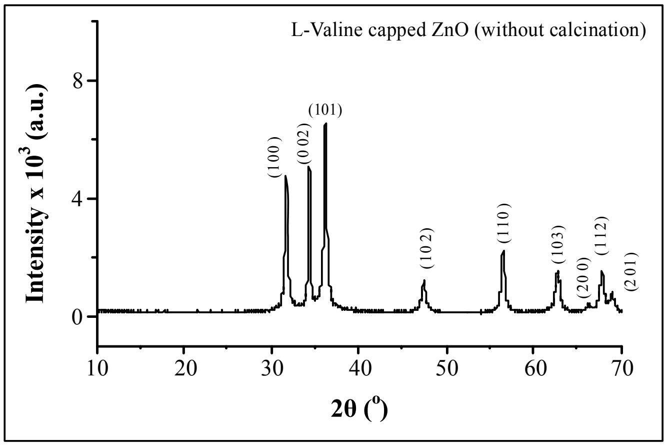

Fig. 4: L-Valine capped ZnO (Without calcination)

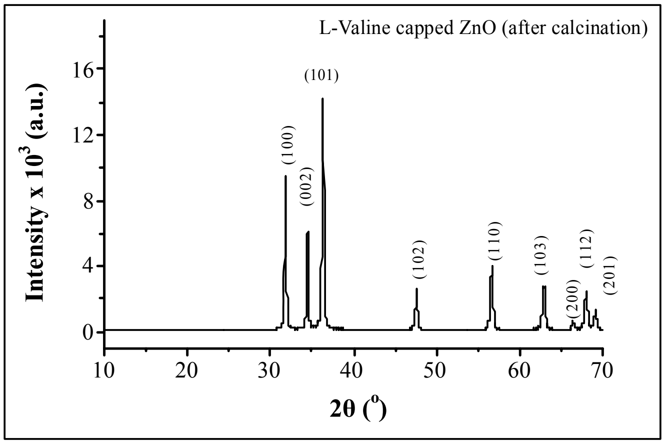

Fig. 5: L-valine capped ZnO (After calcination)

Diffraction peaks are broadened that can be seen from the profile, which confirms the nanocrystalline nature of zinc oxide. XRD pattern also confirms the high purity of nanocrystals as no peak related to impurity is observed[24]. Considering the spherical nature, particle size of these NPs are calculated by Debye-Scherrer formula, $d = k\lambda/(\beta \cos \theta)$; where k is a constant (k = 0.93) and β is width of the diffraction peak at half maxima.

Morphological studies using FESEM and TEM

ZnO NPs capped using L-valine have been subjected to FESEM and TEM. Fig. 6 shows FESEM micrographs and Fig. 7 shows TEM images of ZnO NPs. All micrographs attest the formation NPs having uniform morphology.

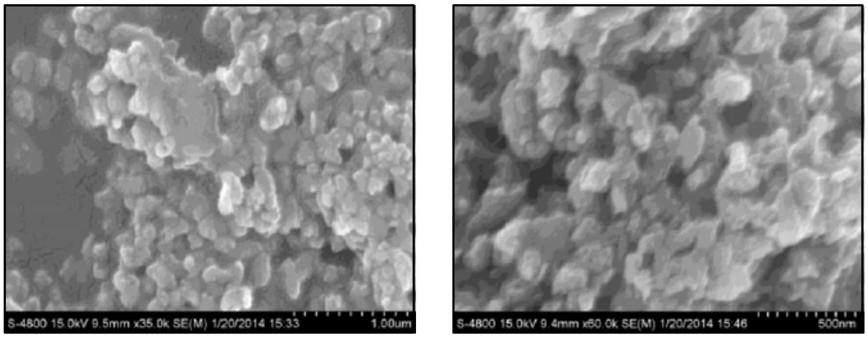

Fig. 6: FESEM micrographs of ZnO NPs

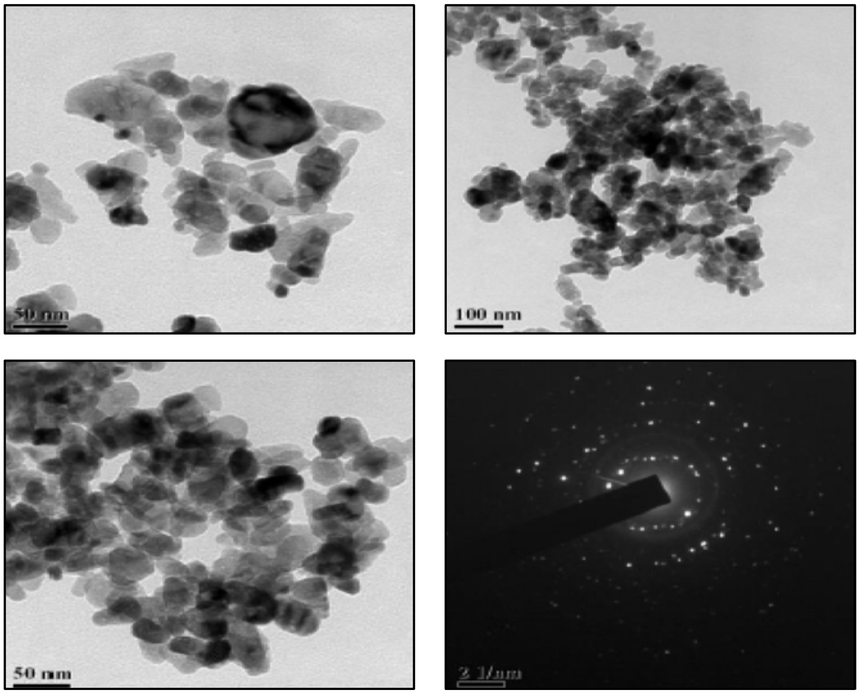

Fig. 7: TEM micrographs of ZnO NPs

CONCLUSION

ZnO NPs were successfully synthesized using L-valine as surface modifying agent. XRD analysis confirms the formation of pure phase hexagonal nanocrystals of ZnO. No impurity peaks were seen in the XRD pattern. By choosing proper concentration of L-valine as a capping agent, particles of narrow size distribution (7 to 8 nm) can be synthesized. After the process of calcination, there is no significant increase in the particle size of ZnO NPs. Particles having such narrow size distribution are capable of showing properties due to quantum size effect and quassi-quantum size effect. The synthesized NPs were characterized by UV-visible spectroscopy and particle size for various samples were calculated using EMA theory. FT-IR analysis confirms the role of L-valine as capping agent. FESEM and TEM investigations attest the formation of ZnO NPs with uniform morphology. Particle sizes calculated using EMA theory and XRD analysis agree with FESEM and TEM images.

ACKNOWLEDGEMENT

Authors are thankful to Director, SRIC, IIT Kharagpur for extending TEM facility and VIT Vellore for XRD facility.

REFERENCES

1. X. Zhong, R. Xie, Y. Zhang, T. Basche and W. Knoll, Chem. Mater., **17**, 4038 (2005).
2. H. Zhong, Y. Zhou, Y. Yang, C. Yang and Y. Li, J. Phys. Chem. C, **111**, 6538 (2007).
3. C. Y. Zhang, H. C. Yeh, M. T. Kuroki and T. H. Wang, Nature Mater., **4**, 826 (2005).
4. R. Agarwal and C. M. Lieber, Appl. Phys. A: Mater. Sci. Process., **85**, 209 (2006).
5. L. Guo, S. Yang, C. Yang, P. Yu, J. Wang, W. Ge and G. K. L. Wong, Appl. Phys. Lett., **76**, 2901 (2000).
6. P. Gaur, D. Sharma, N. Singh, B. P. Malik and A. Gaur, Spectrochim. Acta Part A: Mol. Biomol. Spectro., **97**, 45 (2012).
7. K. Nomura, H. Ohta, K. Ueda, T. Kamiya, M. Hirano and H. Hosono, Science, **300**, 1269 (2003).
8. S. T. Mckinstry and P. Muralt, J. Electroceram., **12**, 7 (2004).
9. Z. L. Wang, X. Y. Kong, Y. Ding, P. Gao, W. L. Hughes, R. Yang and Y. Zhang, Adv. Funct. Mater., **14**, 943 (2004).

10. U. Newmann, R. Grunwald, U. Griedner and G. Steinmeyer, Appl. Phys. Lett., **84**, 170 (2004).
11. J. M. Lin, C. L. Cheng, H. Yu Lin and C. F. Yang Fang, Opt. Lett., **31**, 3173 (2006).
12. L. Schmidt-Mende and J. L. MacManus-Driscoll, Mater. Today, **10**, 40 (2007).
13. G. Shen, J. H. Cho, S. Il Jung and C. J. Lee, Chem. Phys. Lett., **401**, 529 (2005).
14. Y. S. Tamgadge, A. L. Sunatkari, S. S. Talwatkar, V. G. Pahurkar and G. G. Muley, Opt. Mater., **37**, 42 (2014).
15. S. S. Talwatkar, Y. S. Tamgadge, A. L. Sunatkari, A. B. Gambhire and G. G. Muley, Solid State Sci., **38**, 42 (2014).
16. S. S. Talwatkar, A. L. Sunatkari, Y. S. Tamgadge, V. G. Pahurkar and G. G. Muley, Appl. Phys. A, **118**, 675 (2015).
17. Y. S. Tamgadge, V. G. Pahurkar, S. S. Talwatkar, A. L. Sunatkari and G. G. Muley, Appl. Phys. B, **120**, 373 (2015).
18. S. S. Talwatkar, A. L. Sunatkari, Y. S. Tamgadge, V. G. Pahurkar, G. G. Muley, J. Nanostruct. Chem., **5**, 205-212 (2015).
19. J. S. Davies and G. C. Barrett, Amino Acids, Peptides and Proteins, **31**, 1 (2000).
20. D. N. Christodoulides, I. C. Khoo, G. J. Salamo, G. I. Stegeman and E. W. Van Stryland, Nonlinear Refraction and Absorption: Mechanisms and Magnitudes, Advanc. Opt. Photonics, **2**, 60 (2010).
21. L. E. Brus, Electronic, J. Phys. Chem., **90**, 2555 (1986).
22. P. Gaur, D. Sharma, N. Singh, B. P. Malik and A. Gaur, Spectrochim. Acta Part A: Mol. Biomol. Spectro., **97**, 45 (2012).
23. K. Nomura, H. Ohta, K. Ueda, T. Kamiya, M. Hirano and H. Hosono, Science, **300**, 1269 (2003).
24. B. D. Cullity, Elements of X-ray Diffraction, 2nd Ed. Addison-Wesley Publishing Company, Inc. Reading, Massachusetts (1956).

Accepted : 30.11.2015